Available online at www.sciencedirect.com
ScienceDirect
Journal of Electron Spectroscopy and Related Phenomena 155 (2007) 81–85
JOURNAL OF ELECTRON SPECTROSCOPY and Related Phenomena
www.elsevier.com/locate/elspec

Evaporation, fission and auto-dissociation of doubly charged water

E.C. Montenegro [a,*], S.W.J. Scully [b], J.A.Wyer [b], V. Senthil [b], M.B. Shah [b]

[a] *Instituto de Física, Universidade Federal do Rio de Janeiro, Cx. Postal 68528, Rio de Janeiro, RJ 21941-972, Brazil*
[b] *Department of Physics and Astronomy, The Queen's University of Belfast, Belfast BT7 1NN, United Kingdom*

Available online 25 November 2006

Abstract

The paths and mechanisms leading to fragmentation of multiply charged molecules are still not well known. Multiply charged molecules can remain intact, or fragment via evaporation – eliminating light neutral atoms such as H^0 or via fission – ejecting one H^+, or they can breaking up into two or more charged species [S.W.J. Scully, J.A. Wyer, V. Senthil, M.B. Shah, E.C. Montenegro, Phys. Rev. A 71 (2005) 030701(R)]. Small molecules, such as water and methane, are unstable after two or more electron removal. In this work we present experimental results of fragmentation of doubly charged water molecules by 30–1500 eV electrons. We show that, at low energies, doubly charged water essentially undergoes fission but, as the electron energy increases, the complete break-up of water becomes progressively dominant. The contribution to double ionization from auto-ionization [S.W.J. Scully, J.A. Wyer, V. Senthil, M.B. Shah, E.C. Montenegro, Phys. Rev. A 73 (2006) 040701(R)] of singly charged water molecules is discussed.

Keywords: Fragmentation; Water; Electron impact; Ionization

1. Introduction

Molecules ionized by particle impact are often driven to excited states followed subsequently by relaxation through emissions of charged and/or neutral fragments. The charged cations can follow a fragmentation pattern that depends on the ionization state and on how the energy is delivered to the parent molecules. Electron and ion impact can be fast or slow and, in the case of ions, can involve several additional collision channels such as capture of an electron from the target or stripping of an electron from a partially ionized projectile. Each one of these alternatives invokes their own collision dynamics as to how the electrons are removed from the parent molecules and the manner through which the molecules subsequently relax via fragmentation. In face of the complexity of the dynamics involved both in the excitation and the subsequent relaxation processes, it is useful to organize the fragmentation pattern of hydrogen containing molecules by classifying the various outcomes that can arise after final stabilization—do the parent ions remain intact, is there evaporation, i.e. emission of one neutral hydrogen, or is there fission, i.e. one H^+ is released or alternatively do the molecules split into more than two fragment ions? In general the relaxation pattern observed depends strongly on the amount of energy that is transferred to the molecule by the projectile. If the transferred energy is small then there is a large likely hood that the parent molecule ion remains intact, followed by evaporation, fission and splitting, respectively, as the transferred energy becomes higher and higher. Therefore the study of the branching ratios according to the above classification can give some hint about the softness or the hardness of the energy transfer processes.

In this paper we present studies of the fragmentation patterns of water resulting from the formation of singly and doubly charged ions by electron impact along the lines reasoned above. We first briefly describe the experimental set-up and we follow that with a discussion of the patterns observed as one or two electrons are removed from water. For the later, we also consider the role of post-collisional auto-ionization contributions when one inner shell electron is removed during the collision.

2. Experiment

A crossed beam experimental arrangement is utilized in the present work. A beam of electrons composed of narrow pulses of approximately 65 ns in duration with a repetition rate of 10^5 pulses/s crosses a thermal energy beam of a target gas at 90° inside a high vacuum chamber. Extraction pulses applied imme-

* Corresponding author. Tel.: +55 21 2562 7272.
E-mail address: montenegro@if.ufrj.br (E.C. Montenegro).

0368-2048/$ – see front matter © 2006 Elsevier B.V. All rights reserved.
doi:10.1016/j.elspec.2006.11.008

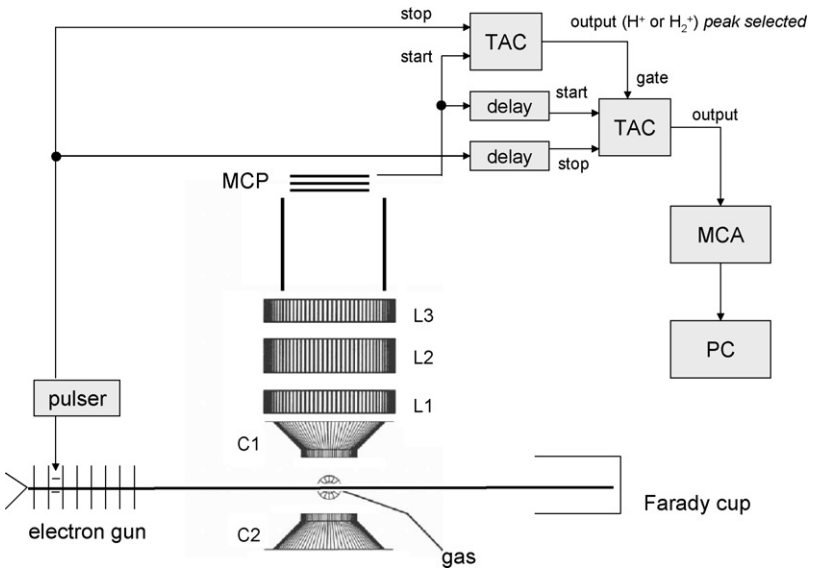

Fig. 1. Schematic diagram of the experimental arrangement showing the electron gun, the time-of-flight spectrometer and the electronics used.

diately following the electron pulses collect any target product ions formed during the transit of the pulses through the target gas. The technique allows ionizing events to be studied in the absence of any electric or magnetic fields and permits the impact energies to be extended down to threshold values without altering any of the collision conditions.

The main features of the experiment are shown in Fig. 1 and have been described previously [1,2]. The interaction region was surrounded by two high transparency grids mounted within the conical electrodes C1 and C2. The target beam was formed in a separate differentially pumped chamber by effusing water vapor gas through a bunch of 1 mm diameter tubes 10 mm in length set within a 4mm diameter tube. The gas pressure in the inlet line was monitored by an MKS Baratron type 170 capacitance manometer and the pressure in the experimental chamber was monitored by an ion gauge. The extracted target ions were guided through a focusing lens system consisting of L1, L2 and L3 into a field free drift region of about 10 cm in length and were detected by a set of three multi-channel plates (MCP). In the present work the 65 ns pulses and a 150 V/cm extraction field was found necessary, in addition to the lens system, to provide the desired high collection efficiencies. The front of the detector assembly was held at a −2.5 kV potential. L1, L2 and L3 were held at −500, −1200 and −500 V, respectively. The time of flight spectra of the target product ions was provided by a time to amplitude converter (TAC) operated with start pulses derived from the extraction pulse generator and stop pulses from the MCP detector. The electron beam energies ranged from 45 to 1500 eV with intensities of 1–30 pA. In order to measure the spectra associated with simultaneous emission of two target ions, a second TAC was gated by the output of the first TAC, set to a window on the H^+ or $H_2{}^+$ ion peak. Therefore, the second TAC only operated when a H^+ or $H_2{}^+$ ion was detected on the first TAC. The start and stop pulses to the second TAC were the same as for the first but were suitably delayed to take account of the signal processing time of the gate signal.

Absolute values of the cross sections were obtained by using CH_4 gas as a target and the methane electron impact cross sections of Straub et al. (σ_{Straub}) [3]. The measured signals, S and S_{coin}, for single ion detection and for two ion detection in coincidence mode, respectively, were normalized to the CH_4 absolute total cross sections through the equation $\sigma_{Straub} = kS/\varepsilon t^2$, where k is the normalization factor, ε the detection efficiency of a single ion and t is the transmission (95%) of each of the two grids used to maintain uniform fields in the extraction/drift region. The efficiency of the MCP detector was determined by measuring the signal at its output and comparing this with the intensity of the signal current measured on the first plate of the MCP. The electron beam intensity was increased by four orders of magnitude to make the later measurement feasible. The efficiency of the detector was determined to be 0.17 ± 0.02. The calculated normalization factor, k, was then used to determine cross section values for the ions produced in coincidence with H^+. Since the coincidence technique involved detecting two particles, each experiencing similar detector efficiencies and grid transmission effects, the detector efficiency and the grids transmission had to be included twice in the coincidence normalization, giving for the coincidence cross section $\sigma_{coinc} = kS_{coin}/\varepsilon^2 t^4$. The $H^+ + OH^+$ or $H^+ + O^+$ doubles pair also contribute to the single ionisation spectra. As the H^+ ions arrive first at the detector, the H^+ ions from these events are recorded with the same 17% detection efficiencies as the singles channel. The contributions of OH^+ and O^+ from doubles pairs in the singles spectra, on the other hand, only happens if the H^+ partner is missed, and are also recorded but with a detection efficiency of 15%. The total OH^+ and O^+ production cross sections reported are corrected accordingly.

3. Single ionization, evaporation and fission

Fig. 2 shows our experimental results for both single and double ionization channels, which were partly presented in Ref. [2]. Compared with previous measurements of single ionization

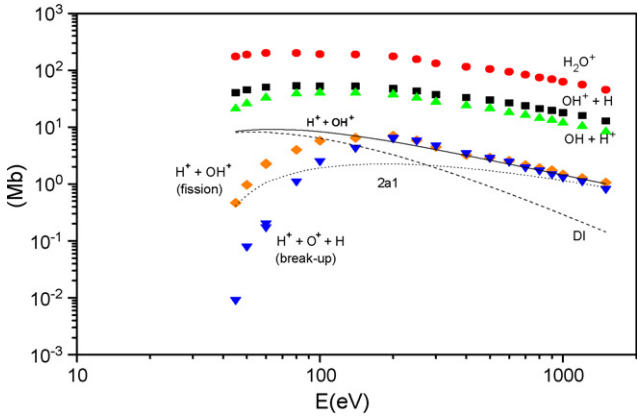

Fig. 2. Measured cross section of products resulting from single ionization (H_2O^+, circles; $OH^+ + H$, squares; $OH + H^+$, up triangles) and double ionization ($H^+ + OH^+$, diamonds; $H^+ + O^+ + H$, down triangles) of water by electron impact. The calculated contributions, taken from Ref. [2], for $H^+ + OH^+$ production are shown by the dashed curve (double ionization, σ_{DI}) and by the dotted curve (post-collisional Auger-like decay following single ionization of the $2a_1$ orbital, σ_{2a1}). The sum of these two contributions is shown by the full curve.

(there are no previous fragmentation measurements for water from double ionization) our normalization procedure gives total single ionization cross sections (sum of all positive products) that are in very good agreement with those reported by Rao et al. [4] and are overall 40% higher than those reported by Straub et al. [5]. The complete set of our measured cross sections are displayed in Table 1. Note that the cross sections for single fragment production in this table are total production cross sections and includes contributions from both single and double ionization channels.

One important point to emerge from Fig. 2 is the behavior of all the cross sections with energy at high collision energies. They all have very similar energy dependence irrespective of whether the cross sections result from single or double ionization processes. If the collision dynamics associated with two electron removal were due to two separate impact processes, then under the independent particle model, they would involve two single ionization probabilities and thus display a faster decrease with increasing projectile energy compared to single electron removal. As discussed by Scully et al. [2], this observed high energy behavior of two electron removal indicates that the dominating process for double electron removal is through a *single* ionization process removing a deep lying $2a_1$ orbital electron followed by a post-colisional Auger-like decay of the excited H_2O^+ molecule to unstable H_2O^{2+} fissionating mainly to the $H^+ + OH^+$ or the $H^+ + O^+ + H^0$ pairs. In the case of $H^+ + OH^+$, the two electron removal is given by $\sigma_{H^+ + OH^+} = A\sigma_{2a1} + B\sigma_{DI}$, where the coefficients A and B are given in Ref. [2]. σ_{2a1} can be determined following the prescription of Hwang et al. [6] and σ_{DI} according the scaling for the isoelectronic systems CH_4 and Ne as given by Luna et al. [7]. These two contributions are shown in Fig. 2 by the dotted and dashed lines, respectively. The sum of these two contributions is given by the full line. A similar calculation can be carried out for the $H^+ + O^+ + H^0$ branch.

In addition to the branching ratio dependence of the fragmentation patterns on energy transfers noted above, the dependence would also be greatly influenced by the momentum transfers, and the electronic states excited during collisions. In Fig. 3 we give a simple method of identifying the relative importance of the various decay modes.

At lower energies the more likely electronic states to be ionized are the non-bonding orbitals $1b_1$ and $3a_1$ and, as a consequence, the cation stabilizes as H_2O^+. As the projectile energy increases, the inner states $1b_2$ and $2a_1$ also become efficiently ionized and, when the electron velocity becomes around three times the average Bohr velocity of these four molecular orbitals, the ionization and the fragmentation ratios become essentially independent of the projectile velocity. Following the results pre-

Table 1
Measured cross sections for fragmentation of water in Mb (1 Mb = 10^{-18} cm^2) leading to total single ion production and total two ion production

E (eV)	H_2O^+	OH^+	O^+	O^{2+}	H_2^+	H^+	$H^+ + OH^+$	$H^+ + O^+$
45	174	40.7	2.67		0.25	21.6	0.47	0.0092
50	188	46.1	3.80		0.27	27.0	0.97	0.080
60	201	52.9	5.48		0.32	35.5	2.29	0.176
80	200	57.4	7.92		0.30	43.9	3.99	1.12
100	192	58.2	9.47		0.30	48.6	5.78	2.55
140	189	59.0	11.4	0.18	0.28	51.1	6.50	4.37
200	175	54.9	11.0	0.27	0.29	50.9	7.09	6.52
250	156	49.0	9.55	0.32	0.25	44.6	5.87	5.89
300	132	41.8	7.82	0.27	0.21	37.1	4.50	4.82
400	115	36.4	6.26	0.22	0.18	30.7	3.26	3.53
500	105	32.9	5.44	0.19	0.16	27.2	2.91	2.92
600	93.8	29.3	4.57	0.17	0.17	23.2	2.57	2.51
700	83.6	25.9	3.90	0.14	0.14	20.5	2.15	1.99
800	74.6	23.0	3.32	0.11	0.12	18.0	1.91	1.75
900	69.4	21.4	3.08	0.11	0.12	16.5	1.75	1.51
1000	62.7	19.4	2.67	0.090	0.10	14.7	1.47	1.33
1200	55.8	17.2	2.37	0.083	0.10	12.8	1.27	1.14
1500	45.4	13.9	1.82	0.071	0.075	10.2	1.03	0.83

Estimated non-systematic uncertainties are 2% for H_2O^+, 5% for OH^+, 7% for O^+, 10% for O^{2+} and H_2^+, 3% for H^+ and 7% for $H^+ + OH^+$ and $H^+ + O^+$.

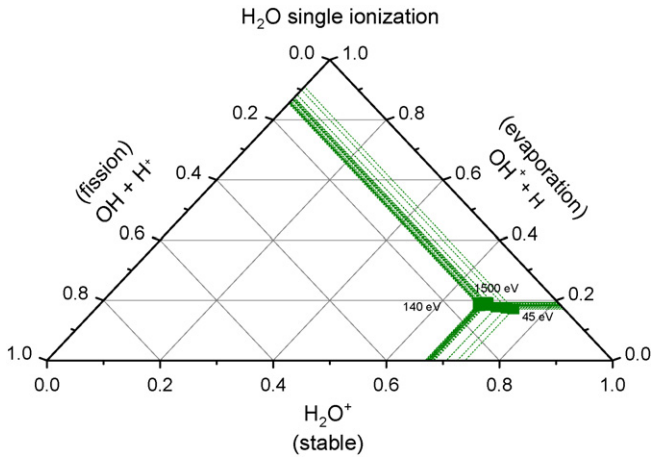

Fig. 3. Ternary graph for the *single* ionization of water by 45–1500 eV electron impact. The figure shows how each of the three main collision products compares with each other. At lower energies the evaporative mode is more likely than the fission mode, but at higher energies both modes compete. However, for all energies the water molecule is more likely to stabilize as H_2O^+ rather than fragment.

sented in Fig. 3, the stable, evaporation and fission branching ratios are ∼68%, 19% and 13%, respectively, for high velocity collisions.

4. Double ionization, fission and break-up

Fig. 4 shows the relative decay modes for double ionization of water. It is clear from the figure that at collision energies near the threshold the main fragmentation is through the fission mode. As the electron velocity increases, the break-up branch $O^+ + H^+ + H$ starts to compete with the fission mode reaching an approximate 50–50 branching ratio for energies above 400 eV. The break-up branch $O^{2+} + H + H$ is always a minor fragmentation mode for double ionization.

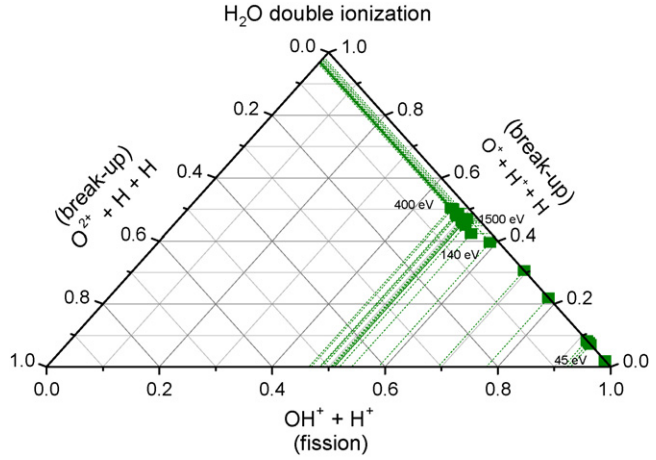

Fig. 4. Ternary graph for the *double* ionization of water by 45–1500 eV electron impact. This figure shows how each of the three main collision products compare with each other. At lower energies the fission mode is more likely than the break-up mode, but at higher energies both modes compete. For all energies it is unlikely that the molecule breaks up releasing O^{2+} as a product.

The observation that the branching ratios for fragmentation at high velocities following double ionization tend towards a fixed value approximately independent of the projectile velocity indicates that the three fragmentation modes presented in Fig. 4 have very similar energy dependence on projectile energy, in a fashion that is similar to single ionization in Fig. 3. Furthermore, as shown in Fig. 2, the energy dependence for double electron removal at high energies, is approximately the same as that for single electron removal. As mentioned above and discussed by Scully et al. [2], this behavior can be explained by contributions emanating from post-collisional Auger-like decay of a single ionized $2a_1$ molecular orbital electron. At high energies the mechanism for double electron removal dominates over the purely two-step ionization process as shown by the dotted and dashed curves, respectively, in Fig. 2. This means that at high velocities, the most probable process of two electron removal involves a $2a_1$ orbital and any one of the three outermost orbitals of the water molecule.

The removal of an electron from the $2a_1$ orbital involves a large energy transfer and, according to Tan et al. [8], results either in the fission or in the break-up of the water molecule. As we show above double ionization at high energies always involves the $2a_1$ orbital and the main fragmentation mode for double ionization is also fission or break-up, as clearly shown in Fig. 4. The general fragmentation pattern for single and double ionization at high energies is diagrammatically illustrated in Fig. 5, where the branching ratios for single ionization is taken from Tan et al. [8] and for double ionization from the present work. The arrows converging to the black dot on the double ionization side represents the origin of the two electrons associated with double ionization: one electron from the $2a_1$ orbital and the other from one of the outermost orbitals.

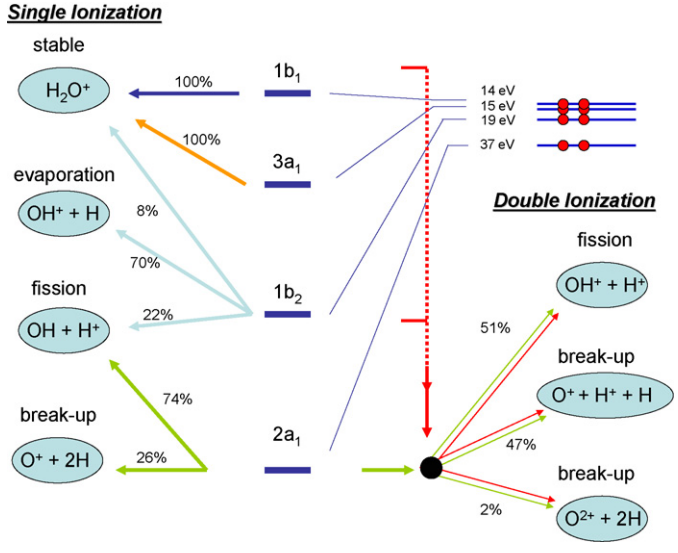

Fig. 5. Diagrammatic representation of the fragmentation pattern of the water molecules for high energy electron impact, following single and double ionization. The left side of the figure shows the branching ratios for fragmentation resulting from electron removal of the identified molecular orbitals. The right side of the figure shows the branching ratios resulting from the removal of one $2a_1$ electron plus one electron from the $1b_2$, $3a_1$ or $1b_1$ orbitals (see text).

5. Conclusions

Although the notion of stabilization, evaporation, fission and break-up might appear a little artificial in a simple molecule like water, they are very useful concepts in larger molecules and aggregates. Because of its small size and importance the water molecule can be used as a starting point in understanding the energetics of molecular fragmentation and the dynamical influences that the energy and momentum transfers exert on the fragmentation pathways of hydrogen rich molecules induced by collisions with electrons, photons and swift ions. For instance with evaporation, there is an increase of the electrostatic energy of the remaining cation (OH^+, in the case of water) because it is now smaller in size compared with the parent ion. This increase is compensated by the decrease in internal energy releasing a neutral H atom. In the fission case, however, there is a decrease in the electrostatic energy resulting from releasing an H^+ ion. Fig. 5 shows that the evaporation is always associated with softer collisions as compared with fission. These relaxation paths combined with the dynamics of the energy and momentum transfers gives the behavior shown in Fig. 3. Indeed, at high energies, the ionization cross sections behaves approximately as $(1/I)\ln(E)/E$ [6], where E is the projectile energy and I the ionization energy of the molecular orbital. Combining this behavior with the fragmentation pathways identified in Fig. 5, the branching ratios for the parent ions remaining stable, dissociating through evaporation or fission are proportional to $(1/I_{3a1} + 1/I_{1b1} + 0.08/I_{1b2}):(0.70/I_{1b2}):(0.74/I_{2a1} + 0.22/I_{1b2})$ giving the values of 71.6%:17.9%:10.5%, not far from the 68%:19%:13% ratios obtained from Fig. 3. In the case of double ionization, the fragmentation dynamics is essentially post-collisional with the $2a_1$ state always involved. Thus, the fission following double ionization involves essentially the dynamics of single ionization of the $2a_1$ state. This explains why in Fig. 2 the $OH + H^+$ and $OH^+ + H^+$ cross sections remain parallel.

Acknowledgments

This work was supported by the Brazilian Agencies CNPq, FAPERJ and CAPES, by the UK Engineering and Physical Science Research Council, by Northern Ireland DEL board and by the IRCEP at Queens University of Belfast.

References

[1] S.W.J. Scully, J.A. Wyer, V. Senthil, M.B. Shah, E.C. Montenegro, Phys. Rev. A 71 (2005) 030701(R).
[2] S.W.J. Scully, J.A. Wyer, V. Senthil, M.B. Shah, E.C. Montenegro, Phys. Rev. A 73 (2006) 040701(R).
[3] H.C. Straub, D. Lin, B.G. Lindsay, K.A. Smith, R.F. Stebbings, J. Chem. Phys. 106 (1997) 4430.
[4] M.V. Rao, I. Iga, S.K. Srivastava, J. Geophys. Res. 100 (1995) 26421.
[5] H.C. Straub, B.G. Lindsay, K.A. Smith, R.F. Stebbings, J. Chem. Phys. 108 (1998) 109.
[6] W. Hwang, Y.-K. Kim, M.E. Rudd, J. Chem. Phys. 104 (1996) 2956.
[7] H. Luna, E.G. Cavalcanti, J. Nickles, G.M. Sigaud, E.C. Montenegro, J. Phys. B 36 (2003) 4717.
[8] K.H. Tan, C.E. Brion, Ph.E. Van Der Leeuw, M.J. Van Der Leeuw, Chem. Phys. 29 (1978) 299.